INFECTION AND IMMUNITY, Mar. 2005, p. 1779–1787 Vol. 73, No. 3
0019-9567/05/$08.00+0 doi:10.1128/IAI.73.3.1779–1787.2005

Phenotypic Switching of *Cryptococcus neoformans* Can Produce Variants That Elicit Increased Intracranial Pressure in a Rat Model of Cryptococcal Meningoencephalitis

B. C. Fries,[1]* S. C. Lee,[2] R. Kennan,[1] W. Zhao,[3] A. Casadevall,[1,4] and D. L. Goldman[5]

Departments of Medicine,[1] Pathology,[2] Urology,[3] Microbiology and Immunology,[4] and Pediatrics,[5] Albert Einstein College of Medicine, Bronx, New York

Received 15 September 2004/Returned for modification 25 October 2004/Accepted 29 October 2004

Increased intracranial pressure (ICP) plays an important role in the morbidity and mortality of cryptococcal meningoencephalitis. The microbial and host factors that contribute to the development of increased ICP are poorly understood. We found that phenotypic switch variants of *Cryptococcus neoformans* (smooth and mucoid) differed in their abilities to promote increased ICP in a rat model of cryptococcal meningitis. Rats infected with the mucoid variant developed increased ICP, whereas rats infected with the smooth parent did not. This trend correlated with a shorter survival time and a higher cerebrospinal fluid (CSF) fungal burden for mucoid variant-infected rats, although brain fungal burdens were comparable between mucoid variant- and smooth parent-infected rats. Magnetic resonance imaging revealed enhanced T2 signal intensity over the surfaces of the brains of mucoid variant-infected rats. In addition, more polysaccharide accumulated in the CSF and brains of mucoid variant-infected rats. The accumulation of glucorunoxylomannan was associated with elevated levels of MCP-1 (CCL2) and, accordingly, a more pronounced but ineffective monocytic inflammatory response in the meninges of mucoid variant-infected rats. In summary, these findings suggest that strain-specific characteristics can influence the development of increased ICP and indicate a manner in which phenotypic switching could influence the outcome of a central nervous system infection.

Cryptococcus neoformans is an encapsulated yeast that causes disease primarily in patients with impaired immunity (13, 38, 42, 45). Cryptococcosis usually presents as chronic meningoencephalitis that is difficult to eradicate, despite antifungal therapy (3, 45). Cryptococcal meningoencephalitis is associated with high morbidity and mortality, especially among immunocompromised hosts (26). Several laboratory indices and symptoms that predict poor outcome have been identified; these include altered mental status at presentation, markedly elevated cryptococcal antigen titers in cerebrospinal fluid (CSF) or blood, and fewer than 20 leukocytes/μl in the CSF (11, 26). In patients with AIDS, significant morbidity and mortality are often a result of increased intracranial pressure (ICP), which can persist even when the cryptococcal infection is controlled. In a large study, elevated ICP (>250 cm of H_2O) was found in about 50% of patients with AIDS in whom this parameter was measured (12, 26, 41).

To date there have been no conclusive studies in humans that relate elevated ICP in cryptococcal meningitis and mortality to the infecting strain of *C. neoformans*. The variability of the inflammatory responses to cryptococcal meningoencephalitis in patients with comparable levels of immunosuppression suggests that pathogen-related factors contribute to the pathogenesis of cryptococcal disease (33, 37). In animal models, differences in virulence among clinical strains have been described for pulmonary infections (2, 17, 19). In addition, the results of several studies have supported the concept that the virulence of a *C. neoformans* strain can be altered by in vitro and in vivo passaging through a process referred to as microevolution (5, 7, 9, 16).

One mechanism for rapid microevolution is phenotypic switching, a phenomenon that generates macroscopically distinguishable colony switch variants which can exhibit differences in virulence from the parent strain (20, 24). We previously described phenotypic switching in several *C. neoformans* strains, including RC-2, a variant of ATCC 24067 (21). The smooth (SM) parent strain generates mucoid (MC) colony phenotype variants at a rate of 0.5×10^{-4} colonies plated. Phenotypic switching of this strain also occurs in mice and is associated with a lethal outcome in immunocompetent mice (21). Thus, phenotypic switching represents a potential mechanism for enhancing virulence during chronic infection. In a murine model of pulmonary cryptococcosis, the MC switch variant is more virulent and fails to elicit an effective granulomatous response. Instead, the MC switch variant elicits a macrophage-dominated inflammatory response, which is associated with extensive lung damage (19, 21). In addition, the MC switch variant sheds a different capsular polysaccharide, which accumulates in the lungs and renders the organism more resistant to phagocytosis by alveolar macrophages.

The objective of the present study was to investigate the virulence of switch variants in a central nervous system (CNS) infection model in rats. We selected the rat model because rats are significantly less susceptible to cryptococcal infection than mice and because the larger size of rats permits better access to CSF and greater definition of CNS structures. Our results demonstrated that the MC switch variant was more virulent in a CNS infection model. Infection with the MC switch variant mimicked the pathogenesis of rapidly progressive CNS cryp-

* Corresponding author. Mailing address: Department of Medicine, Golding 702, Albert Einstein College of Medicine, 1300 Morris Park Ave., Bronx, NY 10461. Phone: (718) 430-3768. Fax: (718) 430-8701. E-mail: fries@aecom.yu.edu.

tococcosis in humans and was characterized by enhanced inflammation, increased accumulation of polysaccharide and, most importantly, increased ICP and decreased survival.

MATERIALS AND METHODS

***C. neoformans* strain.** Strain RC-2 is a variant of serotype D strain ATCC 24067 that originated from the Cherniak Laboratory and presumably emerged from spontaneous microevolution (16). ATCC 24067 was originally obtained from the American Type Culture Collection (Manassas, Va.). Melanization, cell charge, capsule and cell sizes, and sugar assimilation profile for RC-2 were previously described (16, 21). RC-2 was streaked to single colonies and maintained on Sabouraud dextrose agar (SDA [Difco Laboratories, Detroit, Mich.]) plates. RC-2 can produce two colony morphologies on agar, SM and MC, both of which are characteristic of *C. neoformans* colonies (21). The growth of SM and MC colonies in artificial CSF (150 mM Na, 155 mM Cl, 1.0 mM P, 0.8 mM Mg, 1.4 mM Ca, 3.0 mM K) supplemented with either glucose (3.4 mM) or glycine (13 mM) was examined during logarithmic growth phase.

Animal studies. Fischer rats (male, 200 to 250 g) were obtained from the National Cancer Institute (Bethesda, Md.). Anaesthetized rats were infected by inoculation of 100 *C. neoformans* cells in 100 μl of sterile nonpyrogenic phosphate-buffered saline (PBS) into the cisterna magna (intracisternal [i.c.] inoculation) by use of a 26-gauge needle as described previously (23). Dilutions of the infecting suspension were plated on SDA to obtain the number of CFU and confirm that comparable numbers of yeast cells were injected. Rats were observed daily for signs of disease and were killed by lethal injection of pentobarbital. Organ fungal burdens were determined by homogenizing lung and brain tissues in 10 ml of PBS and plating 100-μl samples of the homogenates on SDA. CSF, obtained at the time of killing by puncture of the cistern magna, was also inoculated onto SDA plates. Colonies were counted after 72 to 96 h (one colony represented 1 CFU). All studies were approved by the Animal Care and Use Committee of the Albert Einstein College of Medicine.

Capsule and cell size measurements. The cell and capsule sizes and monoclonal antibody (MAb) staining patterns were examined for unfixed SM and MC cells recovered directly from the CSF of *C. neoformans*-infected rats by two cisternal taps (days 12 and 21). Cells in an India ink suspension were measured at a magnification of ×1,000 under oil as previously described (49). Unfixed cells were stained with a fluorescein isothiocyanate-labeled IgM MAb (12A1) to glucorunoxylomannan (GXM) and then counterstained with Uvitex as previously described (14).

Histological examination and immunohistochemical analysis. To obtain tissues for histological examination and immunohistochemical analysis, rats were anaesthetized and perfused with 4% paraformaldehyde in PBS for tissue fixation under constant pressure, and the brains and lungs were harvested. Tissues were embedded in paraffin, and sections were stained with hematoxylin-eosin or mucicarmine. For macrophage or microglial staining, rabbit anti-Iba1 antibody (Wako Chemicals, Richmond, Va.) was used (30). Briefly, deparaffinized slides were incubated in target retrieval solution (Dako, Carpinteria, Calif.) at 100°C for 30 min. Slides were incubated in 3% H_2O_2 to block endogenous peroxidase and then were treated with 5% goat serum. Rabbit antisera were diluted 1:200 in goat serum and placed on slides for 3 h at room temperature. Slides were incubated with biotinylated goat anti-rabbit IgG at 1:200 for 1 h at room temperature and then with avidin-labeled horseradish peroxidase (Vectastain ABC kit; Vector Laboratories, Burlingame, Calif.). Color was developed with diaminobenzidine (Dako). Tissue immunohistochemical analysis with an MAb (2H1) to GXM was done to detect tissue polysaccharide as described previously (22). For these studies, murine MAb 2H1 (10 μg/ml) was used as the primary antibody. Peroxidase-conjugated goat anti-mouse IgG1 was used as a secondary antibody. The reaction was developed by incubation with diaminobenzidine.

Measurement of GXM in serum, CSF, and brain tissues. GXM levels in CSF and brain tissues were measured by a capture enzyme-linked immunosorbent assay (ELISA) as previously described (23). Briefly, ELISA plates were incubated with rabbit anti-mouse IgM to capture IgM specific to GXM. A standard or a sample (brain homogenate or CSF) was applied, followed by 2 μg of mouse IgG specific for GXM (18B7)/ml. Plates were washed, and bound IgG was detected with alkaline phosphatase-labeled goat anti-mouse IgG. Color was developed with 4-nitrophenyl phosphate, and the absorbance at 405 nm was recorded (39). For studies pertaining to GXM clearance from CSF, rats (five to seven per group) were anesthesized and injected i.c. with 400 μg of GXM dissolved in 100 μl of PBS. GXM was purified from supernatants of SM and MC cultures as described previously (6, 21). Serum was collected at various times after injection for quantification of GXM levels by an ELISA.

Measurement of cytokines and chemokines in brain homogenates. In experiments separate from survival studies, rats were inoculated i.c. with 10^2 SM or MC cells in PBS and killed at 2, 3, or 4 weeks after infection. The brains were removed and homogenized in 5 ml of PBS in the presence of protease inhibitors (complete minikit; Boehringer Mannheim, Indianapolis, Ind.). The homogenates were centrifuged at 6,000 × *g* for 10 min to remove cell debris, and the supernatants were frozen at −80°C until tested. The supernatants were assayed for interleukin-1β (IL-1β) (BioSource International, Camarillo, Calif.) and monocyte chemotactic protein 1 (MCP-1) (CCL2), tumor necrosis factor alpha, IL-4, and IL-10 (BD Bioscience Pharmingen, San Diego, Calif.) concentrations by using commercially available ELISAs.

Measurement of ICP. A 23-gauge cannula filled with 250 U of heparin solution/ml and connected to PE-50 tubing (Intramedic, Becton Dickinson, Franklin Lakes, N.J.) was inserted into the cisterna magna. Tubing was connected by use of a transducer amplifier (Power Lab4/20; ADI Instruments, Milford, Mass.). Recording of pressure and real-time display were performed with a PC (Power Lab software; ADI Instruments). Calibration based on centimeters of water was done before each experiment. As an additional control for these experiments, uninfected (sham) rats were given 100 μl of sterile PBS i.c.

MRI. Magnetic resonance imaging (MRI) was done by use of a scanner operating at 9.4 T (Varian Inc., Palo Alto, Calif.) with a 4-cm-diameter birdcage radiofrequency coil. T2-weighted spin-echo images were obtained by use of a multiecho CPMG imaging sequence (retention time, 2 s; echo time, 20 ms; four echoes) with 13 to 15 imaging slices from the rhinal fissure to the cerebellum. Other imaging parameters were as follows: 30-mm field of view, 128 by 128 pixels (in-plane resolution of 230 μm), and 1-mm slice thickness. Parametric T2-weighted images were created from the signal decay curve of each pixel as a function of echo time.

Statistical analysis. Standard statistical analyses, including Kaplan-Meier, log rank regression, analysis of variance, and *t* test, were performed by using the programs SPSS version 7.5.1 and Microsoft Excel.

RESULTS

The MC variant is more virulent than the SM parent in a rat model of CNS cryptococcosis. (i) Survival. To compare the virulence of the SM and MC phenotypes in a CNS model of cryptococcosis, we infected groups of Fischer rats i.c. with 100 CFU of either SM or MC cells (Fig. 1). The MC switch variant was more virulent than the SM parent, with MC variant- and SM parent-infected rats surviving 21 and 32 days, respectively ($P = 0.03$) (Fig. 1, left panel). Near the time of death, both SM parent- and MC variant-infected rats manifested prostration and hunched backs, clinical signs consistent with meningoencephalitis. The MC variant was also more virulent when higher inocula (10^4 CFU) were used (data not shown). Minor interexperimental variations in median survival (21 to 30 days for MC cells and 35 to > 45 days for SM cells) were observed in repeat experiments with low inocula.

(ii) Fungal burdens. Organ fungal burdens and cytokine and GXM levels were also determined for SM parent- and MC variant-infected rats. These experiments were carried out separately from survival experiments, and there were no deaths in either group. The average brain fungal burden was slightly higher in MC variant-infected rats at 2 weeks, but the average brain fungal burdens were comparable for SM parent- and MC variant-infected rats at 3 and 4 weeks of infection (five rats per group). MC variant-infected rats also exhibited a higher average fungal burden in the CSF than did SM parent-infected rats (Fig. 1, right panel). Both SM cells and MC cells disseminated from the brain to the lungs early in the course of the infection, but MC variant-infected rats had a significantly higher average lung fungal burden throughout the course of the infection (data not shown). The maintenance of the SM and MC phenotypes was verified after plating on SDA. The MC phenotype

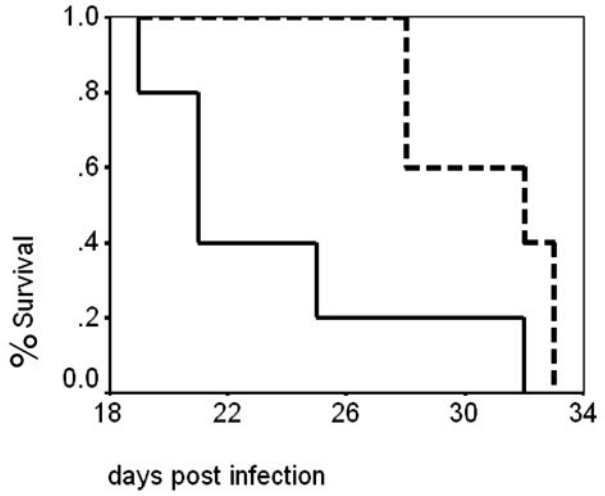

	Time	Smooth	Mucoid	p-value
CSF CFUs	day 12	Log 3.6 ± 0.6	Log 4.7 ± 0.1	P<0.001
	day 14	Log 4.2 ± 0.6	Log 2.3 ± 0.4	P= 0.02
	day 21	Log 4.0 ± 0.6	Log 4.5 ± 0.4	ns
	day 21	Log 4.2 ± 0.2	Log 4.8 ± 0.39	ns
	day 28	Log 4.4 ± 1.0	Log 5.4 ± 0.3	P=0.02
Brain CFUs	day 14	Log 4.5 ± 0.4	Log 5.7 ± 0.4	P=0.002
	day 21	Log 6.1 ± 0.4	Log 5.9 ± 0.36	ns
	day 21	Log 5.4 ± 0.4	Log 5.7 ± 0.2	ns

FIG. 1. (Left panel) Example of survival curves for rats (five per group) infected i.c. with 100 cells of the *C. neoformans* SM parent (broken line) and MC switch variant (solid line) demonstrating the significantly shorter survival of MC variant-infected rats ($P < 0.03$). Repeat experiments demonstrated small variations in median survival but the same difference in virulence. (Right panel) Fungal burdens in brains infected with the SM parent and the MC variant were comparable over the course of the infection, except that the fungal burden was slightly higher in MC variant-infected rats at day 14. In contrast, fungal burdens in the CSF were higher by 0.5 to 2 log units in MC variant-infected rats. ns, not significant.

was unchanged, whereas some MC colonies were recovered from the CSF of one SM parent-infected rat, indicating that in vivo switching can occur in this setting.

Brain weights. Average brain weights at 4 weeks of infection in both SM parent- and MC variant-infected rats were higher than those at 2 weeks or those in uninfected rats. At 4 weeks, the brains of rats infected with the MC variant weighed 6% more than the brains of rats infected with the SM parent (2.06 ± 0.05 [mean ± standard deviation] versus 1.94 ± 0.04 g) ($P = 0.006$). This increase in brain weight was found in repeated experiments and was associated with an apparent increase in brain edema, as indicated by histological examination.

Effects of SM parent and MC variant infections on ICP. We hypothesized that infection with the MC variant may be associated with increased ICP, similar to that observed in humans with rapid progressive CNS cryptococcosis. ICP was measured at 4 weeks after infection by introducing into the rat brain ventricle a 23-gauge needle tip connected to a calibrated pressure transducer. The average ICP of MC variant-infected rats was higher by 7 cm of H_2O than the average ICP of SM parent-infected rats (Fig. 2, left panel). The ICP of SM parent-infected rats was comparable to the ICP of sham-infected rats, and the pressure did not rise before they died (data not shown).

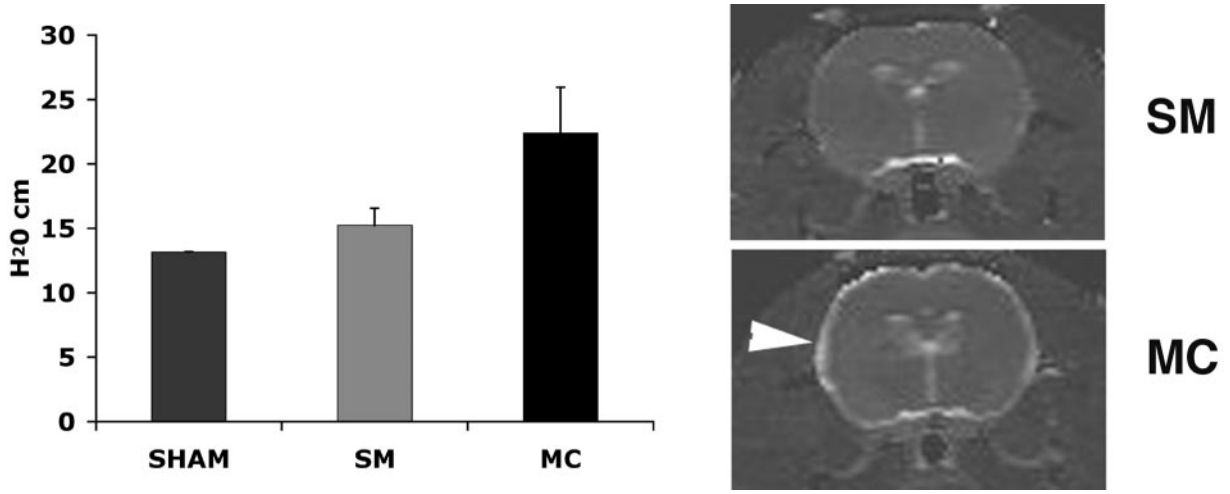

FIG. 2. (A) The ICP was measured 4 weeks after i.c. infection and was found to be significantly higher (P value determined by analysis of variance, 0.03) in MC variant-infected rats than in SM parent- or sham-infected rats. Error bars indicate standard deviations. (B) MRI analysis performed with anesthetized SM parent- and MC variant-infected rats at 3 weeks after infection demonstrated enhanced signal intensity (arrowhead) on T2-weighted images of MC variant-infected rat brains.

MRI. MRI of brains of rats infected with SM and MC cells was performed at 3 weeks after infection. These studies did not show ventricular dilatation for either MC variant- or SM parent-infected rats. T2-weighed images demonstrated increased signal intensity over the surfaces of the brains of rats infected with the MC variant but not the SM parent (Fig. 2, right panel). These findings were consistent with enhanced inflammation, increased accumulation of GXM (see below), increased edema, or a combination of these factors.

Characteristics of inflammatory responses to the SM parent and the MC variant. To further investigate the causes of the increased signal intensity on MRI and the increased ICP, we examined the inflammatory responses by histological examination of brain tissues. Analysis of MC variant-infected brain tissues showed enhanced inflammation within the meninges compared to the results obtained for SM parent-infected brain tissues. Inflammation in MC variant-infected rats was characterized by more pronounced recruitment of mononuclear cells and accumulation of yeast cells (Fig. 3a and b). Immunohistochemical staining for Iba1 (30), a calcium binding adapter molecule that is specifically expressed on monocytes/macrophages and microglia, revealed increased numbers of monocytes/macrophages in the meningeal layers of MC variant-infected rats (Fig. 3c and d). In areas adjacent to the involved meninges, we also noted an increase in highly ramified microglia in the parenchyma of MC variant-infected animals, suggesting increased microglial activation. Brains from MC variant-infected rats also tended to show more edema in the molecular layer and dark shrunken neurons in the underlying cortices (Fig. 3a and b). Of note is that no cells were seen (by direct inspection) in the CSF of SM parent- and MC variant-infected rats at days 12 and 21 after infection. Occasional cryptococcomas were seen in the brains of both SM parent- and MC variant-infected rats. These lesions were typically contiguous with the Virchow-Robin spaces, suggesting direct extension of meningeal disease. The inflammatory response in the lungs of MC variant-infected rats, in association with dissemination, was more pronounced than the inflammatory response in the lungs of SM parent-infected rats (Fig. 3e and f).

Chemokine and cytokine protein expression in infected lung tissues. Next, we measured cytokine and chemokine protein expression in homogenates of brains from SM parent-, MC variant-, and sham-infected rats at 2, 3, and 4 weeks after infection by ELISAs. Significant differences in MCP-1 (CCL2) expression were observed between SM parent- and MC variant-infected rats. MCP-1 levels in brain tissues were about fourfold higher ($P = 0.03$) in MC variant-infected rats than in SM parent-infected rats at 3 weeks after infection (Fig. 4). The same trend was observed earlier in the course of the infection, but the differences did not reach statistical significance ($P = 0.18$). Tumor necrosis factor alpha and IL-1β levels were also increased in both SM parent- and MC variant-infected rats compared to sham-infected rats, but no difference in the expression of these cytokines was observed between SM parent- and MC variant-infected rats. IL-4 and IL-10 levels were not affected by infection. In summary, higher levels of MCP-1 were observed in MC variant-infected rats than in SM parent-infected rats, consistent with an enhanced accumulation of inflammatory cells in the subarachnoid spaces of these rats.

Differences in the accumulation of SM parent GXM and MC variant GXM despite similar fungal burdens. We measured GXM in brain tissues and in CSF at 2, 3, and 4 weeks after infection (five rats per group and time point). GXM accumulated in brain tissues and in CSF over the course of the infection in both MC variant- and SM parent-infected rats. At 2 weeks, GXM was detected in the brains of four of five MC variant-infected rats but in none of five SM parent-infected rats (limit of detection, 50 ng/ml) ($P = 0.048$). At 4 weeks, brain GXM levels were comparable (for the MC variant, 2.4 ± 1.3 [mean ± standard deviation] μg/ml; for the SM parent, 1.8 ± 1.5 μg/ml) ($P = 0.67$). GXM levels increased in the CSF over the course of the infection. At 2 and 4 weeks after infection, GXM concentrations in the CSF were higher in MC variant-infected rats than in SM parent-infected rats (Fig. 5). Maximal CSF GXM levels were 21.8 ± 18.4 and 1.5 ± 1.4 μg/ml in MC variant- and SM parent-infected rats, respectively ($P = 0.02$). Increased accumulation of GXM in tissues was also apparent by mucicarmine staining and immunohistochemical analysis (Fig. 6a to c). The majority of polysaccharide antigen was located in the subarachnoid spaces, where yeast cells and inflammatory cells aggregated (Fig. 6a to c). GXM immunoreactivity was also present in the ventricular and Virchow-Robin spaces and surrounding brain tissues in infected rats. In these regions, GXM immunoreactivity was also greater in MC variant-infected rats than in SM parent-infected rats (data not shown).

Studies comparing capsule induction and polysaccharide clearance in vivo. India ink staining confirmed the accumulation of MC cells in the CSF. Both SM and MC cells exhibited larger polysaccharide capsules in the CSF than under in vitro growth conditions. The capsule radius of MC cells was larger than the capsule radius of SM cells in brain tissues (radius of SM cells, 8 ± 0.5 [mean ± standard deviation] μm; radius of MC cells, 12.3 ± 1.0 μm) ($P < 0.001$). A similar trend was observed in cells from the CSF (radius of SM cells, 9 ± 2.3 μm; radius of MC cells, 11.2 ± 4.2 μm) (P value was not significant). India ink and immunofluorescence staining demonstrated more clumps of aggregated MC cells and clumps of polysaccharide floating in the CSF of MC variant-infected rats (Fig. 6d). The clumps and aggregated cells stained positively for GXM with 12A1, a polysaccharide-specific antibody (Fig. 6e).

To determine whether the increased CSF fungal burdens in MC variant-infected rats reflected differences in growth rates between the strains, we determined growth curves with artificial CSF. These studies showed that SM cells grew more than twice as fast as MC cells in CSF simulated under in vitro conditions (data not shown). These results support the conclusion that decreased clearance of MC cells from the CSF rather than inherent differences in doubling times caused the accumulation of MC cells relative to SM cells.

To further explore the reasons for increased GXM levels in the CSF and brains of MC variant-infected rats, we examined the kinetics of GXM clearance in serum following i.c. injection of GXM. For these experiments, we injected rats (five per group) i.c. with 400 μg of purified SM parent or MC variant GXM. GXM levels were measured over 24 h in the blood and at 24 h in the CSF. These studies showed that both SM parent GXM and MC variant GXM were detectable in serum within

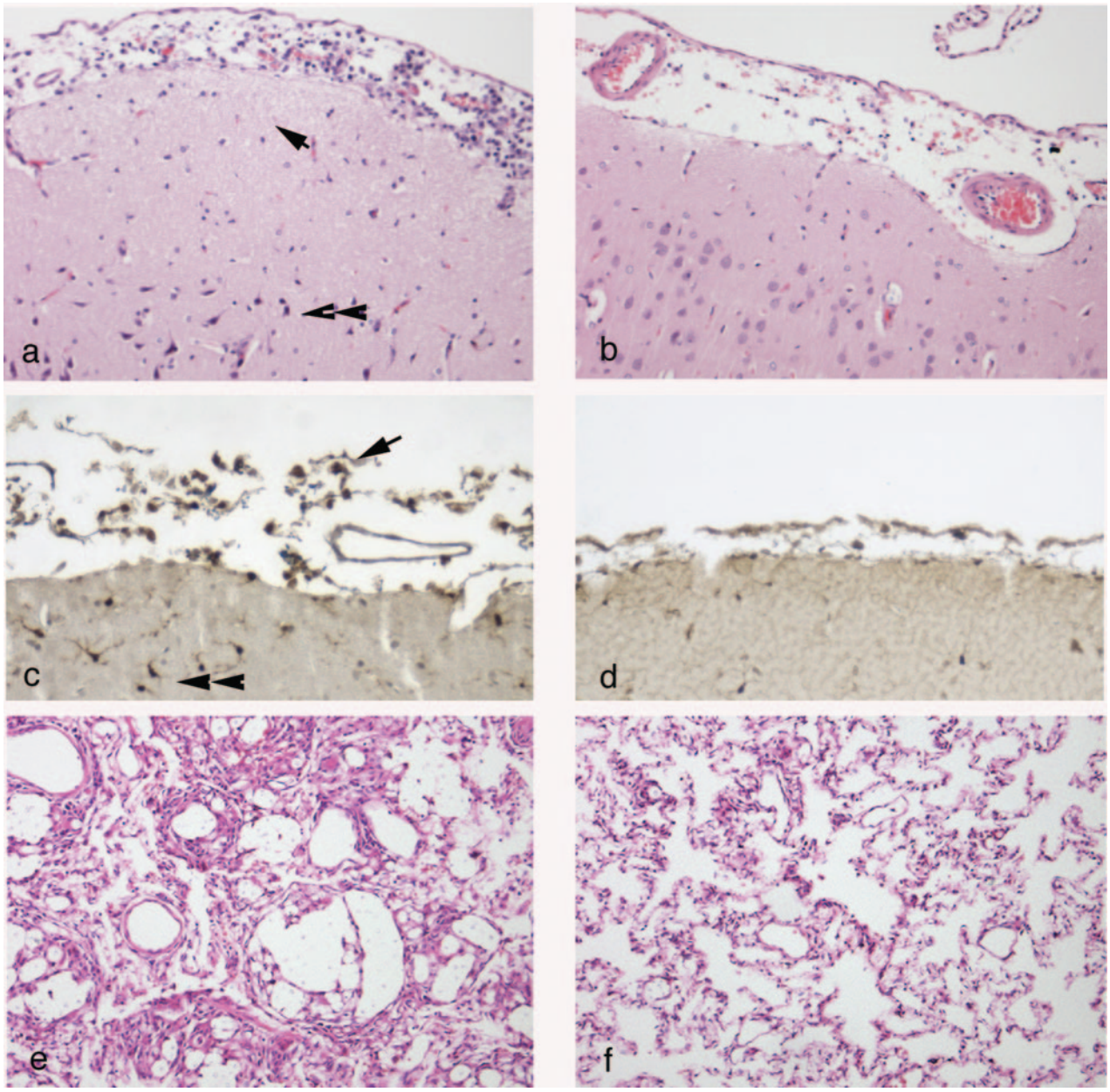

FIG. 3. Histological examination of MC variant- and SM parent-infected rat brains at day 21 (hematoxylin-eosin stain; original magnification, ×100) showed a pronounced mononuclear cell infiltrate in the meningeal layers of MC variant-infected rats (a) compared to SM parent-infected rats (b). The section in panel a also showed edema in the molecular layer (arrow) and dark shrunken neurons in the cortices of MC variant-infected rat brains (double arrowheads). Increased monocyte recruitment was confirmed by immunohistochemical staining for Iba1 (arrow in panel c). In addition, this staining demonstrated more microglial activation in MC variant-infected parenchyma (double arrowheads in panel c) than in SM parent-infected parenchyma (d). Lung tissues also exhibited more inflammation in MC variant-infected rats (e) than in SM parent-infected rats (f) at day 21 (hematoxylin-eosin stain; original magnification, ×100).

2 h of i.c. injection and that over 90% of the GXM was cleared from the CSF by 24 h. Levels of MC variant GXM in serum were significantly higher than those of SM parent GXM at 24 h after injection (13.1 ± 8.2 versus 4.0 ± 2.2 μg/ml) (*P* value determined by *t* test, 0.04). A similar statistically significant difference in GXM levels in serum (data not shown) was obtained in a repeat experiment and may suggest slower clearance of MC variant GXM from the blood. Overall, these studies showed that both polysaccharide capsules are induced in the CSF and that both SM parent GXM and MC variant GXM can exit from the i.c. space to reach the serum compartment; hence, clearance from the CSF may be impaired only in the setting of an inflammatory response.

DISCUSSION

In this study, we investigated the virulence of *C. neoformans* switch variants in a CNS infection model and drew several

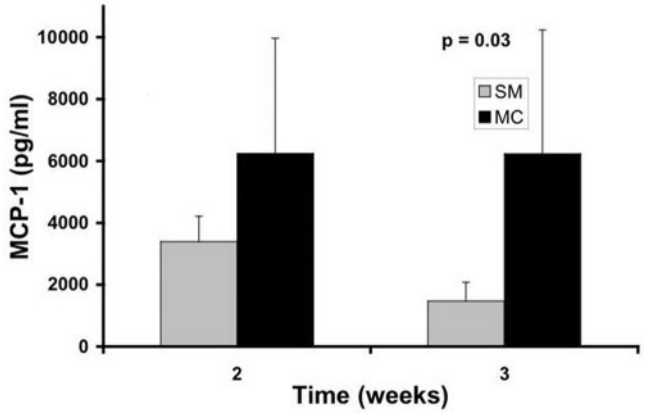

FIG. 4. MCP-1 (CCL2) levels in SM parent- and MC variant-infected rat brains. Columns indicate averages from five rats, and error bars indicate standard deviations. Significantly higher levels were found in MC variant-infected brain tissues than in SM parent-infected brain tissues at 3 weeks after infection. The *P* value was determined by Student's *t* test.

important conclusions. (i) The MC switch variant exhibits enhanced virulence in a rat CNS infection model. (ii) Elevated ICP occurs in MC variant-infected rats but not in SM parent-infected rats. (iii) The elevated ICP in MC variant-infected rats is associated with GXM and yeast cell accumulation predominantly in the CSF. (iv) The enhanced inflammatory response in the subarachnoid spaces of MC variant-infected rats is associated with a higher level of MCP-1 and pronounced recruitment of inflammatory cells. Based on these data, we conclude that phenotypic switching can alter pathogen-related characteristics, which are important determinants in the development of increased ICP.

Elevated ICP in human CNS cryptococcosis is associated with chronic organic brain syndrome, irreversible blindness, deafness (31) and, most importantly, acute mortality in patients with advanced AIDS (26). Interestingly, MC variant-infected rats but not SM parent-infected rats developed increased ICP, implying that pathogen-related characteristics were responsible for the development of the increased ICP. Enhanced virulence was associated with differences in ICP and GXM accumulation but not with sustained differences in brain fungal burdens. Augmented lung fungal burdens in MC variant-infected rats were most likely secondary to decreased clearance of the MC variant from the lungs, analogous to what is seen in pulmonary infection models (21, 27). Although pulmonary involvement may have contributed to the rapid demise (48), several observations suggest that meningoencephalitis was the predominant cause of death; these observations included a hunched back and gait disturbances, both of which are clinical symptoms of meningitis, increased intracerebral pressure, increased brain weight, and histological evidence of cerebral edema and neuron damage.

Cryptococcocal meningitis in humans and rats generally presents as chronic lymphocytic meningoencephalitis (23, 45). Like CSF in humans, CSF in rats is produced predominantly in the choroid plexus of the lateral ventricles and circulates through the third and fourth ventricles into the cisternal space, which is in direct communication with the subarachnoid space.

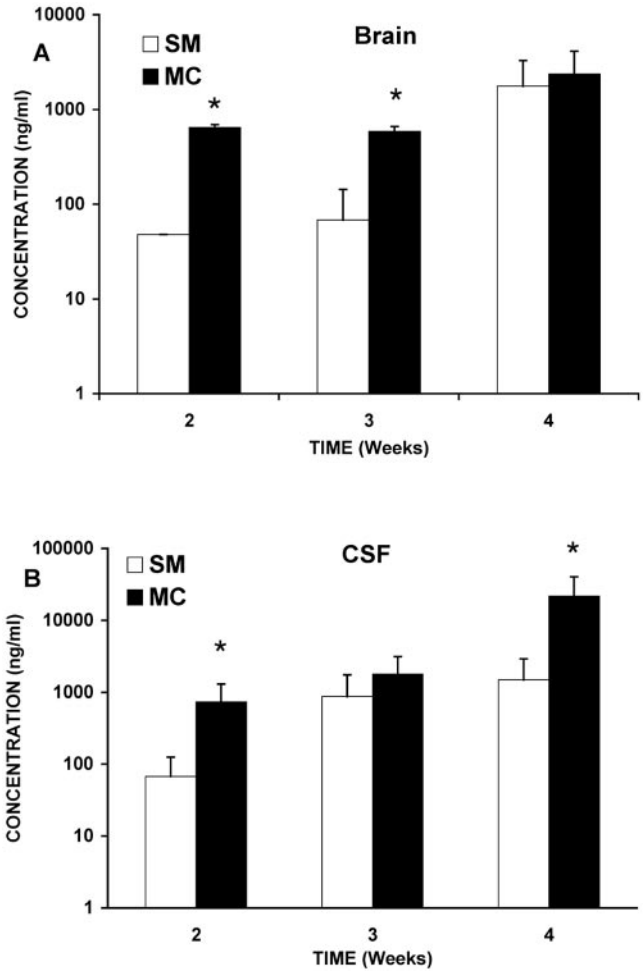

FIG. 5. GXM levels in brain tissues (A) and CSF (B) were determined by ELISAs and were found to be higher in MC variant-infected rats ($P < 0.05$) (asterisks). Columns indicate averages from five rats, and error bars indicate standard deviations.

It has been proposed that elevated ICP in cryptococcal meningoencephalitis results from impaired resorption of CSF in the arachnoid granulations due to the accumulation of cryptococcal polysaccharide and/or organisms (10, 15). Nevertheless, this hypothesis has not been experimentally tested. Impaired CSF resorption resulting in outflow resistance has been suggested by CSF dynamic studies in a single non-human immunodeficiency virus-infected patient with cryptococcal meningitis (29). Impaired CSF resorption has also been demonstrated in animal models of bacterial meningitis (46).

Besides its effects on CSF resorption, cryptococcal polysaccharide accumulation may increase the osmolarity of the CSF and interstitial fluid, thereby promoting brain edema and elevated ICP as a result of the accumulation of extracellular fluid (25). In this regard, Lee et al. have shown extensive GXM deposition in the brains of patients with cryptococcal meningoencephalitis (32). Furthermore, injection of cryptococcal polysaccharide has been shown to result in the accumulation of extracellular fluid within the brain (28).

The MRI study demonstrated the lack of ventriculomegaly consistent with early communicating hydrocephalus, analogous

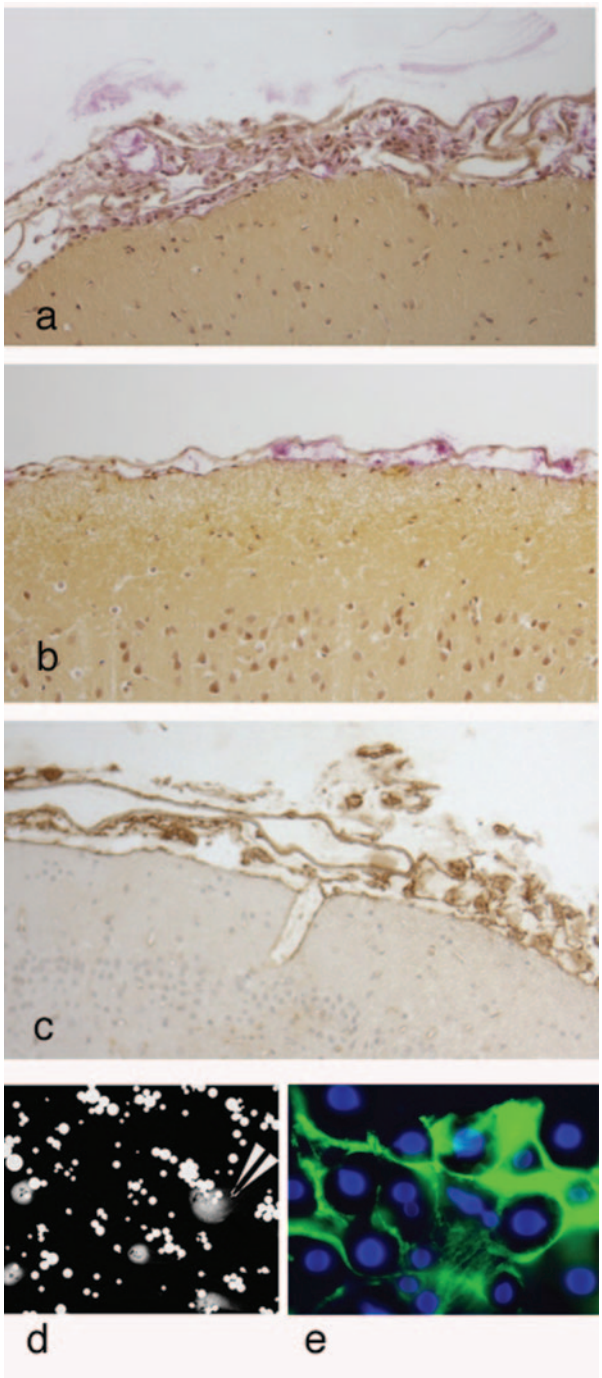

FIG. 6. MC variant-infected (a) and SM parent-infected (b) brain tissues were examined with mucicarmine staining (original magnification, ×100), which revealed an increased accumulation of inflammatory cells in MC variant-infected meningeal cells. Pink denotes polysaccharide. (c) Immunohistochemical analysis (original magnification, ×100) confirmed the presence of GXM in the meninges. (d) India ink staining of CSF demonstrated polysaccharide accumulation and clumping of MC cells (original magnification, ×40). (e) Immunofluorescence staining (original magnification, ×100) confirmed that clumps contained yeast cells (blue) encased in polysaccharide (green).

to what is seen patients with cryptococcal meningitis and elevated ICP (26). Furthermore, enhancement across the convexity of the brain was seen on MRI of MC variant-infected but not SM parent-infected rats. The quality of the scans did not permit a precise diagnosis, but in the context of i.c. infection, our interpretation of these findings was that T2 enhancement reflected either GXM accumulation with brain edema in this area or inflammation or both.

The finding that MC variant-infected rats accumulated more polysaccharide in the CSF and brain tissues parallels the findings in humans, in whom elevated ICP is associated with high cryptococcal antigen titers and yeast cell counts in the CSF (26). Whether enhanced GXM shedding or decreased clearance or both further contribute to the accumulation of polysaccharide is not clear. Nuclear magnetic resonance studies have shown that SM parent GXM and MC variant GXM exhibit the same biochemical repeat structures; however, polysaccharide separation techniques have shown that MC variant GXM and SM parent GXM are different. MC variant GXM is more viscous, inhibits phagocytosis, and appears to promote clumping in the CSF, which may contribute to the development of a more tenacious film of polysaccharide that obstructs the natural passage of CSF across the arachnoid villi (21). In this study, both MC variant GXM and SM parent GXM were cleared from the CSF, similar to the findings of previous experiments with rabbits (1). These studies, however, were done in the absence of inflammation. Histological examination demonstrated an enhanced mononuclear inflammatory response in the meningeal layers of MC variant-infected rats compared with SM parent-infected rats. Most likely this finding was the result of impaired phagocytosis by inflammatory cells in the meningeal layers, consistent with the increased MCP-1 levels and fungal burdens in the CSF of MC variant-infected rats. Growth curves obtained with simulated CSF medium, like growth curves obtained with SDA (21), demonstrated that MC cells grew more slowly than SM cells; hence, the accumulation of MC cells reflected decreased clearance by the host. An enhanced inflammatory response in association with elevated chemokine levels in MC variant-infected animals was also described in murine pulmonary infection models, where it promoted damage and rapid demise (18) (21).

The accumulation of GXM may promote inflammation because GXM can modulate the functions of various inflammatory cells, including leukocyte recruitment to the CNS (34–36, 47). In vitro MC variant GXM and SM parent GXM display different immunomodulatory abilities. These include differential down-regulation of antigen-presenting molecules and differential inhibition of cellular cytokines in human monocytes (44). Hence, it is conceivable that GXM accumulation in the CSF may establish a vicious cycle whereby MC variant GXM elicits an ineffective inflammatory response, which in turn interferes with GXM clearance. Our findings support the notions that, under certain circumstances, *C. neoformans*-related disease is a result of host damage mediated by the inflammatory response (4) and that this process is dependent on the infecting strain.

Among other models (8), the rat model is an established model for CNS cryptococcosis and, as we now demonstrate, this model is ideal for investigations of pathogenesis and potential treatment options for elevated ICP (23). (40, 43). The

potential of *C. neoformans* to induce elevated ICP is dependent on the strain, and rats infected with other variants of ATCC 24067 develop chronic meningitis with granuloma formation and no clinical signs of elevated ICP (23). These data suggest that phenotypic switching of capsular polysaccharides may contribute to the development of elevated ICP and the associated morbidity. We therefore hypothesize that patients who develop increased ICP during cryptococcosis may be infected with cryptococcal strains that produce qualitatively different polysaccharides that inhibit phagocytosis and clearance from the CSF, thereby promoting increased ICP.

ACKNOWLEDGMENTS

We thank Meng-Liang Zhao, Emily Cook, and Frank Bommarito for technical assistance. We also thank George Lantos, the chief neuroradiologist at Jacobi Hospital, for assistance in MRI interpretation.

This work was supported by NIH grants K08-AI01570 and R01-AI59681 to B.C.F. and R01-HL059842 to A.C.; AECOM Center for AIDS Research grant P30AI051519 to S.C.L., A.C., and D.L.G.; and Institute for Smooth Muscle Biology grant HL64547 to W.Z.

The authors of this article have no commercial or other association that might pose a conflict of interest (e.g., pharmaceutical stock ownership or consultancy).

REFERENCES

1. **Bennett, J. E., and H. F. Hasenclever.** 1965. Cryptococcus neoformans polysaccharide: studies of serologic properties and role in infection. J. Immunol. **94:**916–920.
2. **Blackstock, R., K. L. Buchanan, A. M. Adesina, and J. W. Murphy.** 1999. Differential regulation of immune responses by highly and weakly virulent *Cryptococcus neoformans* isolates. Infect. Immun. **67:**3601–3609.
3. **Brandt, M. E., M. A. Pfaller, R. A. Hajjeh, E. A. Graviss, J. Rees, E. D. Spitzer, R. W. Pinner, L. W. Mayer, et al.** 1996. Molecular subtypes and antifungal susceptibilities of serial Cryptococcus neoformans isolates in human immunodeficiency virus-associated cryptococcosis. J. Infect. Dis. **174:** 812–820.
4. **Casadevall, A., and L. A. Pirofski.** 2003. The damage-response framework of microbial pathogenesis. Nat. Rev. Microbiol. **1:**17–24.
5. **Chen, L. C., and A. Casadevall.** 1999. Variants of a Cryptococcus neoformans strain elicit different inflammatory responses in mice. Clin. Diagn. Lab. Immunol. **6:**266–268.
6. **Cherniak, R., L. Morris, B. Anderson, and S. Meyer.** 1991. Facilitated isolation, purification, and analysis of glucuronoxylomannan of *Cryptococcus neoformans*. Infect. Immun. **59:**59–64.
7. **Cherniak, R., L. C. Morris, T. Belay, E. D. Spitzer, and A. Casadevall.** 1995. Variation in the structure of glucuronoxylomannan in isolates from patients with recurrent cryptococcal meningitis. Infect. Immun. **63:**1899–1905.
8. **Chretien, F., O. Lortholary, I. Kansau, S. Neuville, F. Gray, and F. Dromer.** 2002. Pathogenesis of cerebral Cryptococcus neoformans infection after fungemia. J. Infect. Dis. **186:**522–530.
9. **Currie, B., H. Sanati, A. S. Ibrahim, J. E. Edwards, Jr., A. Casadevall, and M. A. Ghannoum.** 1995. Sterol compositions and susceptibilities to amphotericin B of environmental *Cryptococcus neoformans* isolates are changed by murine passage. Antimicrob. Agents Chemother. **39:**1934–1937.
10. **Denning, D. W., R. W. Armstrong, B. H. Lewis, and D. A. Stevens.** 1991. Elevated cerebrospinal fluid pressures in patients with cryptococcal meningitis and acquired immunodeficiency syndrome. Am. J. Med. **91:**267–272.
11. **Dismukes, W. E., G. Cloud, H. A. Gallis, T. M. Kerkering, G. Medoff, P. C. Craven, L. G. Kaplowitz, J. F. Fisher, C. R. Gregg, C. A. Bowles, et al.** 1987. Treatment of cryptococcal meningitis with combination amphotericin B and flucytosine for four as compared with six weeks. N. Engl. J. Med. **317**:334–341.
12. **Dromer, F., S. Mathoulin, B. Dupont, O. Brugiere, L. Letenneur, et al.** 1996. Comparison of the efficacy of amphotericin B and fluconazole in the treatment of cryptococcosis in human immunodeficiency virus-negative patients: retrospective analysis of 83 cases. Clin. Infect. Dis. **22**(Suppl. 2)**:**S154–S160.
13. **Dromer, F., S. Mathoulin, B. Dupont, A. Laporte, et al.** 1996. Epidemiology of cryptococcosis in France: a 9-year survey (1985–1993). Clin. Infect. Dis. **23:**82–90.
14. **Feldmesser, M., J. Rivera, Y. Kress, T. R. Kozel, and A. Casadevall.** 2000. Antibody interactions with the capsule of *Cryptococcus neoformans*. Infect. Immun. **68:**3642–3650.
15. **Fishman, R.** 1992. Cerebrospinal fluid in disease of the nervous system. The W. B. Saunders Co., Philadelphia, Pa.
16. **Franzot, S. P., J. Mukherjee, R. Cherniak, L. C. Chen, J. S. Hamdan, and A. Casadevall.** 1998. Microevolution of a standard strain of *Cryptococcus neoformans* resulting in differences in virulence and other phenotypes. Infect. Immun. **66:**89–97.
17. **Fries, B. C., and A. Casadevall.** 1998. Serial isolates of Cryptococcus neoformans from patients with AIDS differ in virulence for mice. J. Infect. Dis. **178:**1761–1766.
18. **Fries, B. C., E. Cook, A. Guerreo, and A. Casadevall.** 2003. Phenotypic switch switch variants of *Cryptococcus neoformans* differ in virulence in immunocompromised mice, abstr. F54. Abstr. 103rd Gen. Meet. Am. Soc. Microbiol. American Society for Microbiology, Washington, D.C.
19. **Fries, B. C., D. L. Goldman, and A. Casadevall.** 2002. Phenotypic switching in Cryptococcus neoformans. Microbes Infect. **4:**1345–1352.
20. **Fries, B. C., D. L. Goldman, R. Cherniak, R. Ju, and A. Casadevall.** 1999. Phenotypic switching in *Cryptococcus neoformans* results in changes in cellular morphology and glucuronoxylomannan structure. Infect. Immun. **67:** 6076–6083.
21. **Fries, B. C., C. P. Taborda, E. Serfass, and A. Casadevall.** 2001. Phenotypic switching of Cryptococcus neoformans occurs in vivo and influences the outcome of infection. J. Clin. Investig. **108:**1639–1648.
22. **Goldman, D., S. C. Lee, and A. Casadevall.** 1994. Pathogenesis of pulmonary *Cryptococcus neoformans* infection in the rat. Infect. Immun. **62:**4755–4761.
23. **Goldman, D. L., A. Casadevall, Y. Cho, and S. C. Lee.** 1996. Cryptococcus neoformans meningitis in the rat. Lab. Investig. **75:**759–770.
24. **Goldman, D. L., B. C. Fries, S. P. Franzot, L. Montella, and A. Casadevall.** 1998. Phenotypic switching in the human pathogenic fungus Cryptococcus neoformans is associated with changes in virulence and pulmonary inflammatory response in rodents. Proc. Natl. Acad. Sci. USA **95:**14967–14972.
25. **Goldman, D. L., S. C. Lee, and A. Casadevall.** 1995. Tissue localization of *Cryptococcus neoformans* glucuronoxylomannan in the presence and absence of specific antibody. Infect. Immun. **63:**3448–3453.
26. **Graybill, J. R., J. Sobel, M. Saag, C. van Der Horst, W. Powderly, G. Cloud, L. Riser, R. Hamill, W. Dismukes, et al.** 2000. Diagnosis and management of increased intracranial pressure in patients with AIDS and cryptococcal meningitis. Clin. Infect. Dis. **30:**47–54.
27. **He, W., B. C. Fries, A. Casadevall, and D. L. Goldman.** 2000. Phenotypic switch variants, abstr. no. 36. Abstr. 100th Gen. Meet Am. Soc. Microbiol. American Society for Microbiology, Washington, D.C.
28. **Hirano, A., H. M. Zimmerman, and S. Levine.** 1964. The fine structure of cerebral fluid accumulation. IV. On the nature and origin of extracellular fluids following cryptococcal polysaccharide implantation. Am. J. Pathol. **45:**195–207.
29. **Hussey, F., B. Schanzer, and R. Katzman.** 1970. A simple constant-infusion manometric test for measurement of CSF absorption. II. Clinical studies. Neurology **20:**665–680.
30. **Imai, Y., I. Ibata, D. Ito, K. Ohsawa, and S. Kohsaka.** 1996. A novel gene iba1 in the major histocompatibility complex class III region encoding an EF hand protein expressed in a monocytic lineage. Biochem. Biophys. Res. Commun. **224:**855–862.
31. **Johnston, S. R., E. L. Corbett, O. Foster, S. Ash, and J. Cohen.** 1992. Raised intracranial pressure and visual complications in AIDS patients with cryptococcal meningitis. J. Infect. **24:**185–189.
32. **Lee, S. C., A. Casadevall, and D. W. Dickson.** 1996. Immunohistochemical localization of capsular polysaccharide antigen in the central nervous system cells in cryptococcal meningoencephalitis. Am. J. Pathol. **148:**1267–1274.
33. **Lee, S. C., D. W. Dickson, and A. Casadevall.** 1996. Pathology of cryptococcal meningoencephalitis: analysis of 27 patients with pathogenetic implications. Hum. Pathol. **27:**839–847.
34. **Lipovsky, M. M., G. Gekker, S. Hu, L. C. Ehrlich, A. I. Hoepelman, and P. K. Peterson.** 1998. Cryptococcal glucuronoxylomannan induces interleukin (IL)-8 production by human microglia but inhibits neutrophil migration toward IL-8. J. Infect. Dis. **177:**260–263.
35. **Lipovsky, M. M., A. E. Juliana, G. Gekker, S. Hu, A. I. Hoepelman, and P. K. Peterson.** 1998. Effect of cytokines on anticryptococcal activity of human microglial cells. Clin. Diagn. Lab. Immunol. **5:**410–411.
36. **Lipovsky, M. M., L. Tsenova, F. E. Coenjaerts, G. Kaplan, R. Cherniak, and A. I. Hoepelman.** 2000. Cryptococcal glucuronoxylomannan delays translocation of leukocytes across the blood-brain barrier in an animal model of acute bacterial meningitis. J. Neuroimmunol. **111:**10–14.
37. **McDonnell, J. M., and G. M. Hutchins.** 1985. Pulmonary cryptococcosis. Hum. Pathol. **16:**121–128.
38. **Mitchell, T., and J. Perfect.** 1995. Cryptococcosis in the era of AIDS—100 years after the discovery of *Cryptococcus neoformans*. Clin. Microbiol. Rev. **8:**515–548.
39. **Mukherjee, S., and A. Casadevall.** 1995. Sensitivity of sandwich enzyme-linked immunosorbent assay for *Cryptococcus neoformans* polysaccharide antigen is dependent on the isotypes of the capture and detection antibodies. J. Clin. Microbiol. **33:**765–768.
40. **Najvar, L. K., R. Bocanegra, and J. R. Graybill.** 1999. An alternative animal model for comparison of treatments for cryptococcal meningitis. Antimicrob. Agents Chemother. **43:**413–414.
41. **Pappas, P. G., J. R. Perfect, G. A. Cloud, R. A. Larsen, G. A. Pankey, D. J. Lancaster, H. Henderson, C. A. Kauffman, D. W. Haas, M. Saccente, R. J.**

Hamill, M. S. Holloway, R. M. Warren, and W. E. Dismukes. 2001. Cryptococcosis in human immunodeficiency virus-negative patients in the era of effective azole therapy. Clin. Infect. Dis. **33:**690–699.
42. **Perfect, J. R., and A. Casadevall.** 2002. Cryptococcosis. Infect. Dis. Clin. N. Am. **16**:837–874, v–vi.
43. **Perfect, J. R., S. D. Lang, and D. T. Durack.** 1980. Chronic cryptococcal meningitis: a new experimental model in rabbits. Am. J. Pathol. **101:**177–194.
44. **Pietrella, D., B. Fries, P. Lupo, F. Bistoni, A. Casadevall, and A. Vecchiarelli.** 2003. Phenotypic switching of Cryptococcus neoformans can influence the outcome of the human immune response. Cell. Microbiol. **5:**513–522.
45. **Powderly, W.** 1992. Therapy for cryptococcal meningitis with AIDS. Clin. Infect. Dis. **14:**54–59.
46. **Scheld, W. M., R. G. Dacey, H. R. Winn, J. E. Welsh, J. A. Jane, and M. A. Sande.** 1980. Cerebrospinal fluid outflow resistance in rabbits with experimental meningitis. Alterations with penicillin and methylprednisolone. J. Clin. Investig. **66:**243–253.
47. **Vecchiarelli, A.** 2000. Immunoregulation by capsular components of Cryptococcus neoformans. Med. Mycol. **38:**407–417.
48. **Visnegarwala, F., E. A. Graviss, C. E. Lacke, A. T. Dural, P. C. Johnson, R. L. Atmar, and R. J. Hamill.** 1998. Acute respiratory failure associated with cryptococcosis in patients with AIDS: analysis of predictive factors. Clin. Infect. Dis. **27:**1231–1237.
49. **Zaragoza, O., B. C. Fries, and A. Casadevall.** 2003. Induction of capsule growth in *Cryptococcus neoformans* by mammalian serum and CO_2. Infect. Immun. **71**:6155–6164.

Editor: T. R. Kozel